· Article · Advances in Polar Science
doi: 10.13679/j.advps.2019.0003 June 2019 Vol. 30 No. 2: 118-131

# Modified Rammsonde tests in layered compacted snow

ZHUANG Feng[1], LU Peng[1*], LI Zhijun[1], HAN Hongwei[2] & LI Wei[1]

[1] State Key Laboratory of Coastal and Offshore Engineering, Dalian University of Technology, Dalian 116024, China;
[2] School of Water Conservancy and Civil Engineering, Northeast Agricultural University, Harbin 150030, China

**Received 14 February 2019; accepted 25 May 2019; published online 25 June 2019**

**Abstract** Investigation of the physical and mechanical properties of snow has long been a topic of interest to researchers as the construction of compacted-snow runways in Antarctica developed. In an attempt to assess the strength of layered compacted seasonal snow, penetration tests using modified Rammsonde were conducted in Harbin, China in early 2018. Compared with previous models, the modified Rammsonde is lighter overall, with improved resolution; thus, it is more suitable for seasonal snow; the mechanical structure was adjusted, and the reading of depth data is more convenient. A total of 74 penetration tests were carried out and the results were analyzed both qualitatively and quantitatively. The results of these analyses demonstrated the applicability of the device, and revealed that several factors affect the cone penetrometer's estimate of the strength of the layered compacted seasonal snow. Such factors include the confining pressure, penetration energy, and the snow material properties, particularly the compaction of the snow undergoing penetration. A linear relationship between the penetration pressure and snow density was also established. The effect of age hardening on the penetration pressure was studied and the microstructure of the snow particles was observed through a microscope. These analyses showed that the cone penetrometer and data processing methodology applied in this study enable a rapid estimate of strength in seasonal snow, and may be applied in Antarctica after further modification. This would provide a scientific basis for the design of China's Antarctic ice sheet airport.

**Keywords** layered compaction, penetration, resistance, snow hardness, snow age hardening

**Citation:** Zhuang F, Lu P, Li Z J, et al. Modified Rammsonde tests in layered compacted snow. Adv Polar Sci, 2019, 30(2): 118-131, doi: 10.13679/j.advps.2019.0003

## 1 Introduction

The Antarctic continent, which is covered with snow and ice, is a vast and inhospitable territory, affected by changeable weather conditions. Land transportation on the continent is time-consuming and dangerous due to the presence of snow and ice crevasses. As China's Antarctic Kunlun Station is located more than 1000 km from the coast, the use of land transport convoys to the station is very tedious and perilous. The conduct of polar science relies on polar infrastructure and many countries have realized that infrastructure limitations are undermining their polar scientific capabilities (McCallum, 2018). Therefore, countries such as the United States, Russia, Britain, or Germany have been using aircraft on the Antarctic continent over the past few years. China has been using helicopters for many years for various aerial operations in its Antarctic expeditions. However, the increasing technical and logistical demands for the growing number of scientific missions conducted by China's Antarctic expeditions require the use of airplanes, such as China's first polar fixed-wing aircraft, Snow Eagle 601 (Gao et al., 2018), for conducting such works. As the use of wheeled, rather than ski-equipped aircraft is preferable, and because most natural snow-covered areas are not suitable for the operation of such aircraft, the snow needs to be processed to obtain sufficient bearing capacity for the wheeled aircraft (McCallum, 2012, 2014). Therefore, investigation of the physical and mechanical properties of snow has long been a

* Corresponding author, E-mail: lupeng@dlut.edu.cn

topic of interest to researchers.

Generally, the strength of snow can be described as compressive, tensile or shear, but it is also often expressed in other terms based on *in situ* measurements, such as hardness or resistance. Snow hardness is the resistance to penetration or the pressure required to penetrate the snow, and is measured by a penetrometer. Similar to snow strength, it is the bonding between the snow grains that determines the penetration resistance. Consequently, the resistance depends on the shape of the snow crystals and their orientations, both of which influence the nature of the bonds between the crystals. The overall penetration resistance generally increases with depth due to compaction by the weight of the overlying layers. As with most snow properties, the resistance is constantly changing under the influence of processes such as sintering —where the number and size of the bonds between the ice grains increases with time—and compaction, both of which result in densification. As these two mechanisms typically occur over time, the increase of snow hardness with time is expected (Moser and Sherwood, 1967; Schaerer and McClung, 2006; McCallum, 2012).

The first penetrometer used for snow, called Rammsonde, was developed by Haefeli (Bader et al., 1939). This instrument is used for measuring the resistance of snow with depth based on the penetration of a cone under the impact of known energy, and is suitable for low to very high hardness measurements. The Rammsonde is a simple, sturdy, and portable instrument which can be used with little training (Schneebeli and Johnson, 1998); thus, it is the most commonly used instrument in field measurement for determining the nature of snow strength and monitoring the age-hardening process (Shoop et al., 2010). Although other penetrometers have been developed since the implementation of the Rammsonde, it is still the only instrument capable of measuring an index of the snow mechanical properties, that is widely accepted in the scientific community and can be used in polar regions (Perla and Martinelli, 1975; McCallum 2012, 2014).

To answer the needs of the Chinese Antarctic expeditions, a proper protocol for testing the snow mechanical properties should be established. Based on the national needs and the background of lack of experience in the construction of polar snow projects and relevant snow mechanical tests, a series of experiments are needed first. Therefore, prior to conducting tests in the challenging conditions of Antarctica, a site in Harbin, in northeastern China, was chosen for testing the reliability of instruments and data processing methods. The cone penetrometer used in this paper is a modified version of the dynamic cone penetrometer used in soil mechanics, and its structure and principle are similar to those of the Rammsonde. Because the Rammsonde was designed for use in the polar environment, which is characterized by a relatively high snow strength, the size and weight of the Rammsonde components make it inadequate for use on seasonal snow, which has lower density and hardness. Therefore, some modifications of the weight and size of the penetrometer were made. The purpose of this paper is to assess the reliability of the modified cone penetrometer and data processing methods, and to provide a rapid measure of strength in seasonal snow, before possibly deploying the instrument in Antarctica after further modification, thus providing a scientific basis for the design of China's Antarctic ice sheet airport.

After a brief description of the instrument and the principles underlying snow strengths measurements (Section 2), the validation of the device through *in situ* tests is conducted and described in Section 3. In Section 4 we discuss the influence of the penetration energy on hardness measurements, and introduce a linear relationship between penetration resistance and density. The effects of age hardening on resistance are also investigated in Section 4 through a comparative analysis of the test results, and the microstructure of snow particles, observed and documented through the microscope, are described. Concluding remarks are provided in Section 5.

# 2 Theory and test methods

## 2.1 Preparation of snow samples

Many attempts were made by various nations to establish runways from processed snow, and techniques for building such runways have been in place for more than 50 years. Among them, layered compaction is an effective method developed to improve the strength of snow, and it has been applied to the construction of runways in Antarctica. Compared with single-layer snow, the increased thickness reduces the average unit strength required to support a given load, and layered compaction prevents isolated areas of low-strength snow in the lower layers from affecting the overall strength of the structure (Moser and Sherwood, 1967).

The layered compaction method was used on snow samples in the Northeast Agricultural University campus in Harbin from January 14 to February 6, 2018, during a period of frequent snowfall. The test site was surrounded by high buildings on three sides, forming a large area of shadow and little wind. The maximum accumulated snow cover in the test site was about 15 cm, and the snow for the test was prepared from the fallen snow on the ground. Soft, undisturbed snow on the upper layer was collected to avoid the effect of sintering and compaction, and any hard lumps were removed. Then, the snow samples were prepared by layered compaction in wooden boxes (0.15 m × 0.15 m, 0.6 m high) according to the following protocol: The complete amount of snow was divided into six parts, each part becoming a 10-cm-thick layer of snow. The mass of each layer equaled the product of its volume and the design density. The snow of each layer was placed in the wooden box after weighing, then tamped periodically with an iron plunger (made by welding a 2-cm-thick square metal plate

to a 60-cm-long metal tube) to a height of 10 cm, as shown in Figure 1a. This was repeated six times to obtain a box of layered snow with a depth of 60 cm. This process allows test samples of nearly constant density to be prepared (Gow and Ramseier, 1964). Penetration tests were carried out immediately after the snow samples were prepared. The tests were conducted in the wooden boxes described above. The ambient temperature and snow temperature were measured by thermometer before each test, and did not exceeded −8℃ throughout the test period. Therefore, the snow can be treated as a two-phase material consisting of ice and air, similar to polar snow (McCallum, 2012). Both the ambient temperature and snow temperature showed great fluctuations, though.

A total of 74 penetration tests were conducted; the test details are listed in the Appendix Table 1.


**Figure 1** **a**, Preparation of snow samples; **b,** Penetration test in progress.

## 2.2 Theoretical model of snow under penetration

Snow can be regarded as a cellular form of ice, in which the individual ice crystals of snow are bonded together (Petrovic, 2003). This microstructure gives strength to snow, but also determines its rheology. The Mohr-Coulomb criterion has been used in snow mechanics since scientists began to investigate the subject (Mellor, 1975); it describes the relation between the shear strength of a material and the applied normal stress and can be expressed as:

$$\tau = C + N\tan\phi \quad (1)$$

where $\tau$ is the shear strength, $C$ is the cohesion, $N$ is the applied normal stress and $\phi$ is the friction angle of the material.

Mellor (1975) stated that the idea of treating snow as a $C-\phi$ material is attractive, as $C$ can be identified with the time-dependent (sintered) intergranular bonding, and $\phi$ can be thought of as characterizing the initial strength of the disaggregated snow and the residual strength after bonds have been broken. There may be cases involving processed snow where this concept is useful, but it is questionable whether internal friction can be fully mobilized until $C$ is effectively destroyed. Therefore, Mellor (1975) suggested that snow (at least on the microscale) is possibly best described as either a cohesive or a frictional material rather than a cohesive and frictional material. On this basis, Martin (1997) proposed that the cohesive strength predominates any mobilized frictional strength, and is later replaced by the frictional strength when cohesion is lost.

Based on the above, McCallum (2012) proposed to apply the Mohr-Coulomb criterion in the behavior of snow during penetration, and assumed that before the bonds are broken the snow has cohesion but no friction (as no inter-particle movement has occurred), and immediately after the penetration test, bonds are fractured, and the snow will be in a particulate state where it has friction but no cohesion. Thus, following the Mohr-Coulomb criterion, the shear strength of the snow is assumed equal to the cohesion of the snow prior to failure, and post-failure the shear strength (assuming no immediate re-sintering of particles) is considered a function of the friction between the fractured particles and normal stress.

The Mohr-Coulomb criterion was also applied in this paper to interpret the behavior of snow during penetration. The snow described in Section 2.1 was almost fresh snow which was collected during a period of frequent snowfall; we therefore assumed that the snow was almost unbonded, and the resistance to cone penetration will come largely from friction between the grains. For the snow discussed in Section 4, which sintered for days after compaction, bonds had begun to form and grow; hence, we assumed that the resistance to cone penetration came from cohesion and friction successively.

## 2.3 Structure and operation of penetrometer

The cone penetrometer used in this study was modified from a dynamic cone penetrometer used in soil mechanics, so its design and principle are similar to those of the Rammsonde. The Rammsonde is suitable for polar environments, so its components are large and heavy as the strength of polar snow is relatively high. Seasonal snow does not usually reach the density and strength of polar

snow. Thus, it is too soft to even support the weight of the instrument itself, and the penetrometer shaft may penetrate deep into the snow without being hammered. Therefore, for low-density snow a larger cone is used with a diameter of 120 mm and an angle of 120° (Wong and Irwin, 1992). The change in the size and angle of the cone tip in turn affects the hardness measurement which requires complicated conversion when comparing data from different cones (Wong and Irwin, 1992). Thus, the modification for Rammsonde is mainly aimed at reducing its size and weight to make it more suitable for seasonal snow.

The cone penetrometer includes five main parts: a hollow, 16 mm-diameter high-strength steel shaft with a 60° conical tip, a guiding rod with a metal disk, a positioning bolt, a drop hammer, and a steel ruler (Figure 2). The guiding rod is screwed onto the top of the shaft and guides the drop hammer. The shaft can be lengthened with threaded extensions according to the thickness of the snow deposition. The guiding rod, hammer, shaft and extensions are all made of high-strength steel. The cone tip has a diameter of 20 mm and a height of 17 mm; the total length of the penetrometer cone element (to the beginning of the shaft) is 54 mm. To reduce sidewall friction, the penetrating head design has a diameter slightly larger than the shaft. The probe with its shaft, and the guide rod with its metal disk and positioning bolt have a mass of 1.19 kg and 1.68 kg, respectively. Two drop hammers, weighing 1 kg and 2 kg, are used.

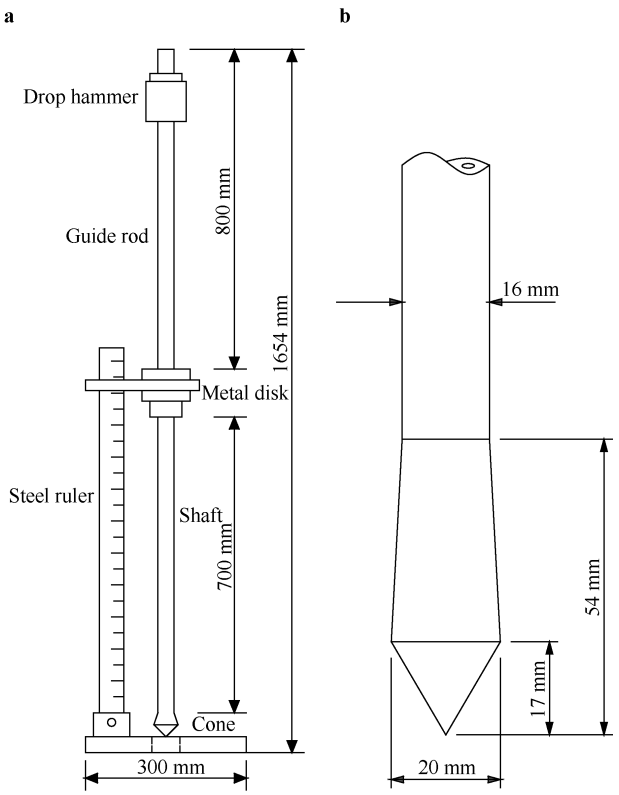


**Figure 2** **a**, Cone penetrometer; **b**, Close-up view of the cone.

Compared with the previous models, the modified Rammsonde is lighter overall, thus more suitable for seasonal snow; the resolution is improved; depending on the penetration energy and snow material properties, the maximum resolution can reach 5 mm while that of the original Rammsonde is only 10 mm (McCallum, 2012). The mechanical structure was adjusted—an added metal disk makes it more convenient to read the depth data.

To make a measurement, the hammer is raised by hand to a certain height which is marked by the positioning bolt on the guide rod, and then dropped freely. The penetration depth is read from the steel ruler beside the shaft. The resistance to penetration (also referred to as hardness) of the snow can be determined by observing either the amount of penetration after each hammer drop or the number of hammer drops (blows) necessary to obtain a certain penetration. In relatively hard, homogeneous snow it is usually more convenient to determine the number of blows needed to penetrate through some predetermined depth increment; recording the number of hammer blows after each 5-cm depth increment is a convenient, commonly used procedure. In layered and new, soft snow, however, observing the amount of penetration after each hammer blow is a more suitable procedure (Shoop et al., 2010).

The combination of appropriate hammer weight and drop height (from 0 to 30 cm) usually allows for a suitable rate of penetration (between 20 to 30 hammer blows per minute) to be obtained in a great variety of snows. Typically, using fewer hammer weight and drop height combinations during the tests means more efficient subsequent data processing (Shoop et al., 2010).

## 2.4 Calculation of snow hardness

The resistance or hardness is computed from the following expression:

$$R = \left( \frac{Whn}{x} + W + Q \right) \cdot \alpha \tag{2}$$

where $R$ is the resistance (kg), $W$ is the weight of the drop hammer (kg), $h$ is the drop height (cm), $n$ is the number of hammer blows, $x$ is the penetration depth after $n$ blows (cm), $Q$ is the weight of the penetrometer (kg), and $\alpha$ is a correction factor. When using the Rammsonde, because of the conical shape of the penetrometer head and the vicinity of a free surface, the correction factor $\alpha$ is 4.7 for depths of 0 to 5 cm, 1.6 for depths of 5 to 10 cm, and 3 for depths of 0 to 10 cm, to obtain the true hardness of the 10-cm surface layer; and $\alpha$ = 1 beyond 10 cm depth (Shoop et al., 2010). Same factors are used in this paper because the same conical angle and tip shape as those of the Rammsonde are used.

The hardness $R$ is an index which indicates the resistance in kilograms presented by the snow to the vertical penetration caused by ramming a metal cone of any known dimensions (Shoop et al., 2014) on the snow surface. The

resistance reading at any depth (obtained when the tip of the cone is located at this depth) represents the mean hardness through the depth increment between this and the previous reading. In equation (2) small energy losses related to the elastic losses in dropping the mass, and the friction between the tubes and the snow forming the sides of the hole (Gubler, 1975), are neglected.

To obtain the pressure–depth relationship, the unit of resistance $R$ should be converted into $N$, then converted into pressure $p$ by dividing the resistance $R$ by the projected area of the cone, using the following expression:

$$p = \frac{R \cdot g}{A} \tag{3}$$

where $p$ is the penetration pressure, in Pa; $R$ is the resistance in kg; $g$ is the gravitational acceleration in $m \cdot s^{-2}$; and $A$ represents the projected contacted area of the cone base in $m^2$ (Wong and Irwin, 1992).

## 3 Validation tests

To assess the validity and repeatability of the data obtained by our penetrometer, several groups of validation tests were conducted, and their results were compared with those documented by previous studies using a Rammsonde. Such studies are abundant, due to the extensive use of the instrument.

Eight different validation experiments were conducted with a snow density of 550 $kg \cdot m^{-3}$, and the weight and falling height of the hammer set to 2 kg and 10 cm (tests 1–5), and 2 kg and 20 cm (tests 6–8). The penetration pressures obtained from these eight experiments are plotted as a function of depth in Figure 3, together with results from three similar tests conducted by Shoop et al. (2010) as part of a snow road field assessment program near McMurdo Station, Antarctica, during the 2002–2003 austral summer. The Rammsonde was used to conduct *in situ* measurements of the strength of the snow roads. Although the snow density was variable, Shoop et al. (2010) selected locations with higher density uniformity (density varying between 550 and 600 $kg \cdot m^{-3}$, with layers deeper than 15 cm being higher in density). Because their results were provided in kgf, the penetration resistance needed to be converted to pressure according to equation (3) prior to analysis. It should be noted that the weight and falling height of the hammer were not documented in the literature.

In many cases, the pressure–depth relationship measured by our penetrometer and the Rammsonde showed similar characteristics, with pressure values of the same order. The depth-varying pressure trends are different, though. The curves of the eight experiments are similar and show good repeatability. Therefore, the data obtained using the cone penetrometer and Rammsonde were regarded as comparable, considering the possible differences in the properties of the snow, the atmospheric conditions and the confining pressure.

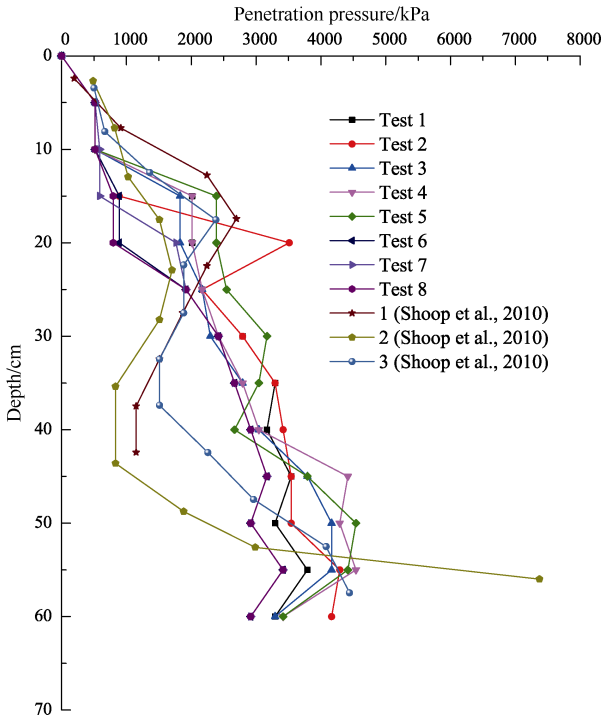


**Figure 3** Penetration pressure as a function of depth from eight validation tests (tests 1–5, 6–8) and from Rammsonde measurements in Antarctica (Shoop et al., 2010).

The influence of the confining pressure on the resistance has to be considered because the penetration tests of this study were conducted in wooden boxes to control the density. Consequently, additional groups of penetration tests were carried out in wooden boxes of different sizes: Box A (0.25 m × 0.25 m × 0.6 m, tests 9–13), Box B (0.15 m × 0.15 m × 0.6 m, tests 14–18) and Box C (0.09 m × 0.09 m × 0.6 m, tests 19–23) with same hammer weight and drop distance (2 kg, 10 cm) and for a snow density of 500 $kg \cdot m^{-3}$. Figure 4 displays the depth–penetration pressure results of the group-averaged tests (Boxes A, B, C). The resistance values measured in Box B and Box C are considerably larger than those in Box A, which is consistent with the rationale for a possible increase in resistance as the confining pressure is increased (Renshaw and Schulson, 2001), while the resistance values are not the largest in Box C with the largest confining pressure. We note that for depths shallower than 20 cm, little difference exists between the three curves, whereas for depths greater than 20 cm, the penetration resistance increases with depth in the two smaller wooden boxes (Boxes B and C). Conversely, the penetration resistance in the larger box (Box A) only fluctuates slightly between 1100 and 1600 kPa at larger depths. The possible explanation for this difference is that as the lateral pressure increases in the smaller box, crack initiation (required for brittle failure) was restricted and greater resistance was achieved (Renshaw and Schulson, 2001). However, this effect seems to decrease significantly in surface snow regardless of the confining pressure

because the existence of a free surface and sufficient pore space in porous (lower density) snow ameliorate this effect and enables unhindered fracture and compaction (McCallum, 2012). Hence, although the confining pressure may have some impact on the tip resistance of the snow, the variation was complicated by the density and microstructure of the material, and analysis of the available data was inconclusive.

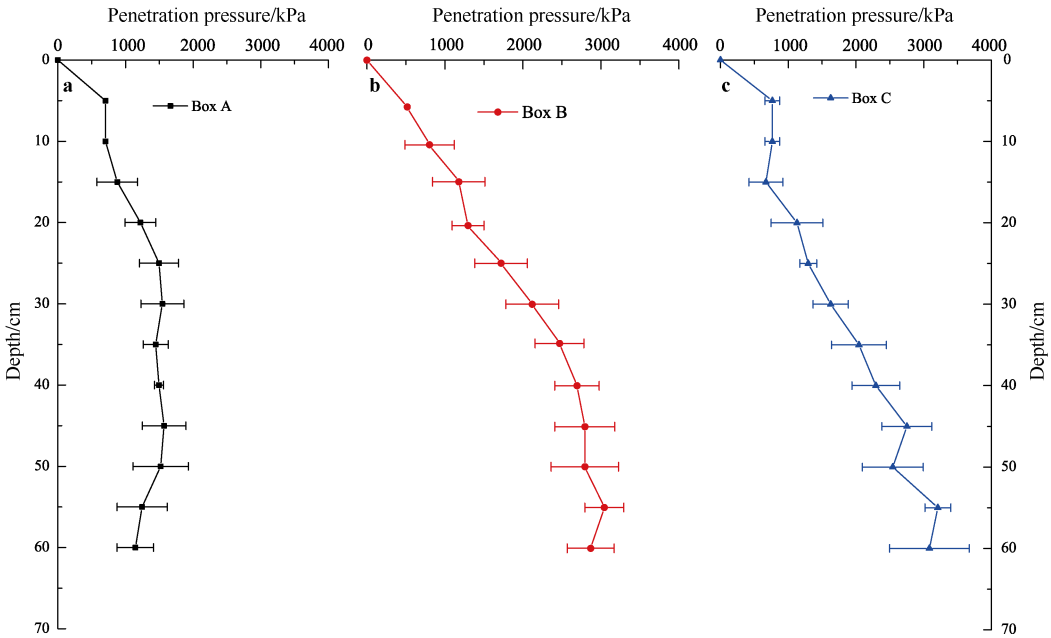


**Figure 4** Penetration pressure as a function of depth for group-averaged data in wooden boxes of different sizes. **a**, Box A (0.25 m × 0.25 m, 0.6 m high); **b**, Box B (0.15 m × 0.15 m, 0.6 m high); **c**, Box C (0.09 m × 0.09 m, 0.6 m high).

# 4 Results and discussion

## 4.1 Effect of penetration energy

Further tests were conducted to evaluate the effects of the penetration energy on the resistance estimates. The penetration tests were carried out in snow with a density of 450 kg·m$^{-3}$, with a hammer weight of 1 kg and drop distances of 15 cm (tests 24–28), 20 cm (tests 29–33), 25 cm (tests 34–38) and 30 cm (tests 39–43). The results (penetration pressure as a function of depth) of these four groups of tests are averaged per group and shown in Figure 5.

Additional penetration tests were carried out in snow with a density of 500 kg·m$^{-3}$, with a hammer weight of 2 kg and drop distances of 10 cm (tests 14–18), 15 cm (tests 44–48) and 20 cm (tests 49–53). Figure 6 shows the group-averaged penetration pressure as a function of depth for each group.

Obviously, as the penetration energy increases, the standard deviation of the hardness measurements decreases gradually, which indicates that the measured hardness values are more accurate and reliable. Table 1 summarizes the variations in the average pressure values across various tests, for different penetration energies, for snow of two different densities. The mean penetration pressure under different penetration energies was different. The results in Table 1 clearly show a decreasing penetration pressure trend as the drop height increased, whereas such a decrease was not systematically observed when the overall penetration energy increased. These tests demonstrate that when the weight of the hammer was held constant and only the drop height, i.e. kinetic energy changed, the pressure values changed for snow of equal density. Therefore, the influence of penetration energy should be considered when comparing the results of various tests.

Mellor (1975) stated that the Rammsonde penetration resistance $R$ has the dimensions of force, but it actually represents the driving energy per unit penetration for a fixed cross-sectional area $A$ of the penetrometer point; therefore, $R/A$ can be interpreted as the specific energy required for penetration. During penetration, the energy is expended in breaking bonds, displacing material laterally, and compacting in an annular zone around the penetrometer hole (Mellor, 1975). It is thus easy to understand that when the snow density changes, or the number and size of bonds between the grains changes, the energy required to penetrate to a certain depth is different. However, the energy that Mellor (1975) refers to is actually different from the penetration energy that we discussed earlier. $R/A$ can be regarded as the real energy transfer from the shaft to the snow, while the penetration energy mentioned before is the total energy, which includes energy losses. The greater the penetration energy, the more real energy is transmitted to

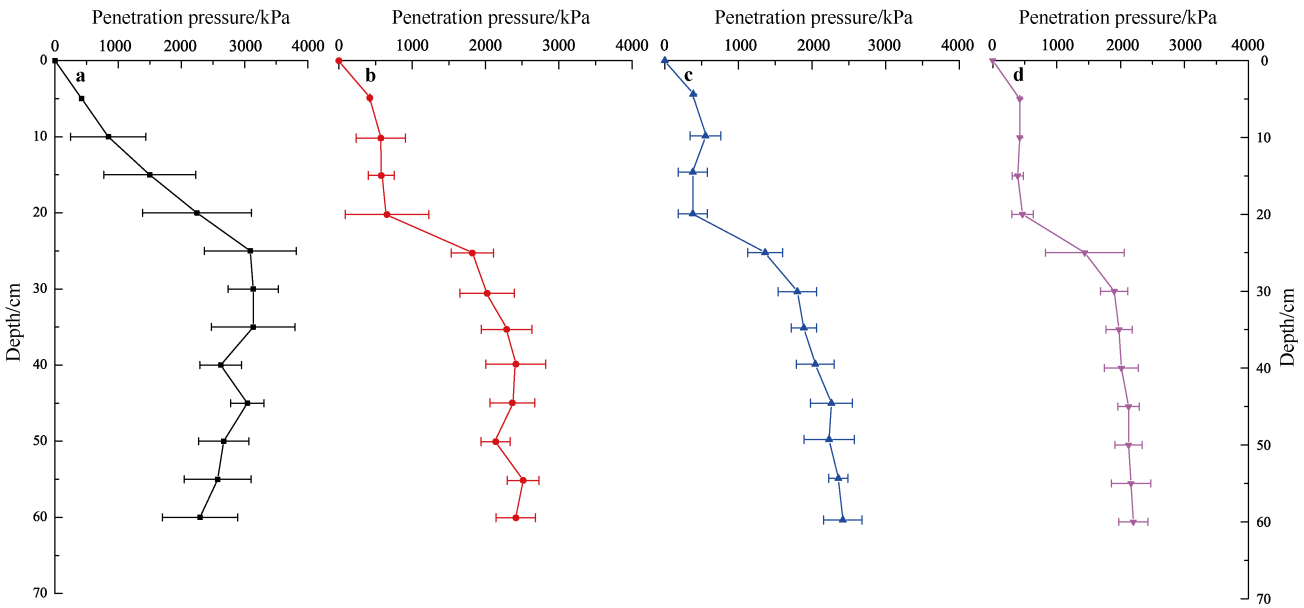


**Figure 5** Penetration pressure as a function of depth, for four different penetration energies (tests 24 – 43). **a**, 1 kg, 15 cm; **b**, 1 kg, 20 cm; **c**, 1 kg, 25 cm; **d**, 1 kg, 30 cm.

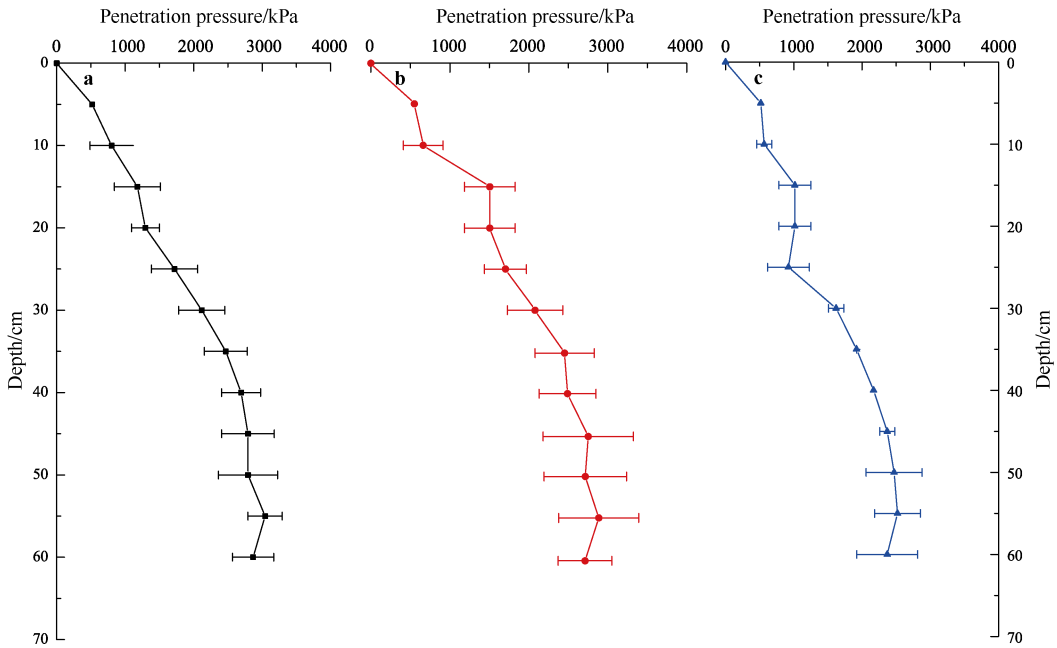


**Figure 6** Penetration pressure as a function of depth, for three different penetration energies (tests 14–18, 44–53). **a**, 2 kg, 10 cm; **b**, 2 kg, 15 cm; **c**, 2 kg, 20 cm.

the snow. But more energy is not always better, and vice versa. For low-density snow, excessive penetration energy may cause the penetrometer to move straight to a large depth, even down to the bottom of the layer after one or a few impacts. This distorts the results, which then cannot reflect the true resistance or hardness. For snow of high density, a penetration energy too small will cost more time and effort because penetration to the same depth will require more impacts. In this case, the main value of this test would be impaired because the advantage of the cone penetration testing lies in its simplicity of performance and evaluation. It is therefore necessary to choose an appropriate penetration energy or a uniform drop weight and distance when measuring hardness or resistance under different conditions. Niedringhaus (1965) and Waterhouse (1966) also noticed the influence of penetration energy on snow hardness measurements. After further study, Waterhouse (1966) proposed a new hardness formula which takes into account the influence of different hammer weights. But the correction Waterhouse (1966) offered is

complex, it has not been used in practice and is not applied in this study. In technical reports of CRREL, the impact of penetration energy was not considered, which merits further study.

**Table 1** Penetration pressure as a function of penetration energy, i.e. hammer weight and drop height

| Test | Density /(kg·m$^{-3}$) | Weight and drop height of hammer | Mean penetration pressure/kPa |
|---|---|---|---|
| 24–28 | 450 | 1 kg, 15 cm | 2298.29 |
| 29–33 | 450 | 1 kg, 20 cm | 1687.85 |
| 34–38 | 450 | 1 kg, 25 cm | 1493.30 |
| 39–43 | 450 | 1 kg, 30 cm | 1470.44 |
| 14–18 | 500 | 2 kg, 10 cm | 2024.49 |
| 44–48 | 500 | 2 kg, 15 cm | 1968.84 |
| 49–53 | 500 | 2 kg, 20 cm | 1622.41 |

### 4.2 Relationship between measured pressure and initial density

The properties of snow usually analyzed are the density, grain size, crystal form and degree of compaction; generally, the annual layering can be determined from the density profile alone (Bull, 1956). Density is also the most commonly used property in relation to other mechanical parameters. The usual way to get a complete and accurate density profile is to dig a snow pit, which has the advantage of providing information other than density via direct examination, but is a time-consuming process. A more convenient method for acquiring a density profile is the penetration test, although it does not provide a direct observation of the snow layers and their density. The snow hardness correlates approximately with the density of the snow, and low hardness may be an indicator for layers of low density. This section aims to quantifying the relation between snow density and penetration test data.

Penetration tests were conducted on homogeneous snow of various densities (tests 1–5, 14–18, 54–68) with a hammer weight of 2 kg, and a drop height of 10 cm. The weight and height were chosen after analysis of the results of multiple experiments with different penetration energies under different densities.

The results of these tests suggest a direct relationship between the initial density and the depth-averaged tip resistance (Figure 7). The regression equation for density on resistance (with the units given above, and assumed to be a pure numbers), is

$$p = 15.95\rho - 5997.13 \quad (4)$$

obtained with a coefficient of determination $R^2 = 0.95$.

The equation curve from Bull (1956) in Figure 7 was determined from, and is applicable to, natural high-density snow (density 420–570 kg·m$^{-3}$) of the Greenland Ice Sheet, using a Rammsonde. Although both curves show a tendency of rising resistance as the density increases, there are differences between the data and fitted curve, which can be attributed to variations in the snow properties. The snow tested by Bull (1956) was the annual accumulation of snow in a permanent snow field, with a maximum snow depth of more than 10 m. Only after a considerable period of natural compaction, accompanied by sintering, can natural snow reach such a high density. The bonds formed between the grains by sintering generally grow with time, increasing the strength of the snow. Because of the existence and fracture of the bonds, the resistance to penetration is provided by cohesion and friction successively, as described in Section 2.2. Lower temperatures (−22℃– −32℃) may also have contributed to Bull's results. The snow tested in this paper was almost fresh snow, which is normally mostly unbonded. Different densities were achieved by using an iron plunger and layered compaction. Once volumetric deformation and close-packing has been achieved, it is more difficult to displace the fractured particles laterally and compact the particles ahead of and to the side of the cone; thus, the snow has increased resistance to any imposed stress (McCallum, 2012). Although both curves show similar tendencies, they are actually reflections of different internal mechanisms. Gubler (1975) also studied the relationship between hardness and density, although the density involved was too low (below 350 kg·m$^{-3}$) to be applicable to high-density snow. This was also the case for the resistance–density relationship obtained by Schneebeli and Johnson (1998) using Snow Micro Penetrometer. Other experimental data obtained by Rammsonde confirm the close relationship between density and hardness, but as most of them did not control density, the relationship between hardness and density within a larger density range has not been obtained.

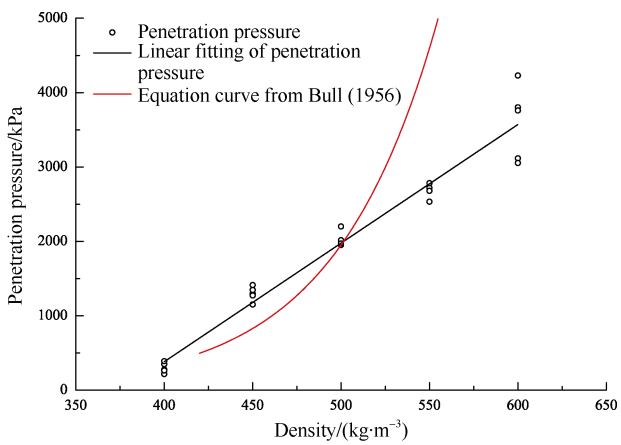


**Figure 7** Depth-averaged pressure for each test versus initial density.

The tests conducted in this study were aimed at demonstrating that a direct relationship exists between the penetration pressure and initial density of snow or a firm layer, and that based on that relationship an accurate density profile can be deduced from the hardness profile. It should

be noted that equation (4) only applies to snow that has just been layered and compacted, because the time variation in the microstructure of snow of similar density yields significantly different values of resistance or pressure (Kirchner et al., 2001). The bonds between the individual snow crystals depend on the microstructure. They grow over time after the deposition in a process called sintering. Thus, sintering will increase the strength of the snow with time, while the density does not increase at the same rate. Even so, this does not mean that equation (4) has no practical significance or that density data are not important. On the contrary, density or density stratification of newly compacted snow can be obtained by equation (4), which can be used to assess the degree of snow compaction. And although many factors, such as atmospheric conditions, snow material properties and especially the compaction of the snow undergoing penetration, affect the resistance, a similar relationship may exist in polar snow (Bull, 1956). In this sense, more work is needed to find the relationship between density and penetration resistance or pressure in different snow metamorphic processes. Monitoring of the snow strength during and after the construction of the runway will establish the feasibility of creating snow of adequate strength to support the aircraft or vehicles that can effectively make deliveries to the Antarctic. On the other hand, it may be preferable to use resistance with or without additional density data as an index property for the mechanical properties of snow (Swinkels, 2017), because resistance, rather than density, can truly reflect the microstructural changes caused by sintering and the resulting increase in strength (Mellor, 1975; Shapiro et al., 1997; Schaerer and McClung, 2006). Moreover, resistance has been shown to be correlated well with the elastic modulus (Swinkels, 2017) and other strength indicators, such as compressive strength (Fukue, 1997) and tensile strength (Borstad and McClung, 2011).

### 4.3 Effect of age hardening

Studies have shown that the nature of snow varies over time (Wuori, 1963; Gow and Ramseier, 1964; Colbeck, 1987; McCallum, 2012), a process known as age hardening. To investigate the effect of age hardening, five penetration tests (tests 49–53) were conducted in snow compacted to 500 kg·m$^{-3}$, then a series of penetration tests was carried out after placing the snow samples outdoors for 72 h, 120 h and 168 h, respectively. The weight and falling height of the hammer were 2 kg and 20 cm, respectively. Consistent with the literature (Abele, 1990; Blaisdell et al., 1998), the effects of snow age hardening, which manifest as an increase of the penetration pressure with time, were detected, as shown in Figure 8. Table 2 summarizes the variation in average pressure values across various tests, after different aging hours, within snow of identical initial density.

The increase in pressure is caused primarily by the processes of sintering, whereby the number and size of the bonds between the ice grains increases.

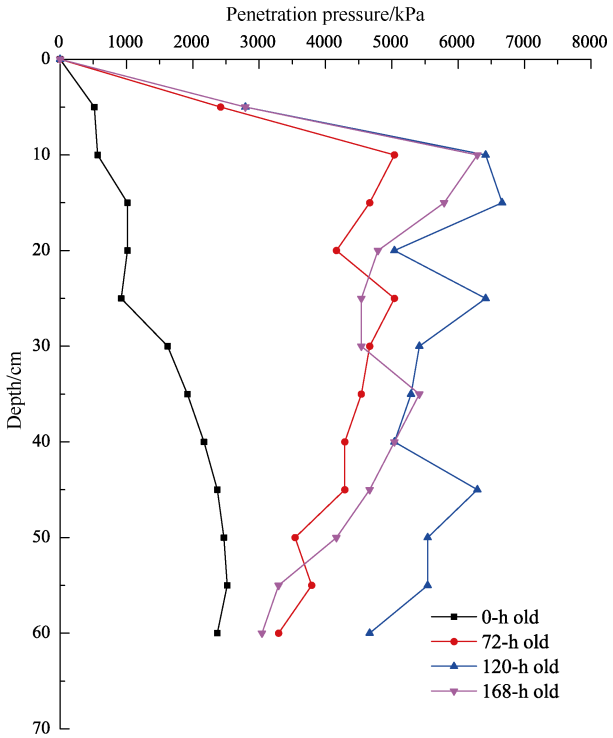


**Figure 8** Penetration pressure as a function of depth at different stages of aging.

**Table 2** Summary of penetration pressure as a function of age hardening

| Test | Age/h | Mean penetration pressure/kPa |
|---|---|---|
| 49–53 | 0 | 1622.41 |
| 69–70 | 72 | 4146.07 |
| 71–72 | 120 | 5425.68 |
| 73–74 | 168 | 4530.99 |

Results of field studies on the changes in snow structure with aging were reported by Gow and Ramseier (1964), Colbeck (1987) and Hong (2014). Changes occur shortly after the snow is deposited, when the process of sintering begins. All these studies indicated that snow age hardening involved the formation of bonds between grains, and that the strength of the snow seemed to be determined mostly by the number and size of the inter-granular bonds. Wuori (1963) showed that 50% of the optimum strength gain was typically achieved 72 h after compaction. The remaining 50% strength gain was reached after 28 d, assuming temperature fluctuations were limited (Melendy and Shoop, 2017). The process of age hardening is illustrated by images of snow particles observed under a microscope (Figure 9) at different stages of aging. Another process, compaction, that may lead to increased pressure and which results in densification, is not noticeable as the changes in the overall height of the snow samples were less than 2%.

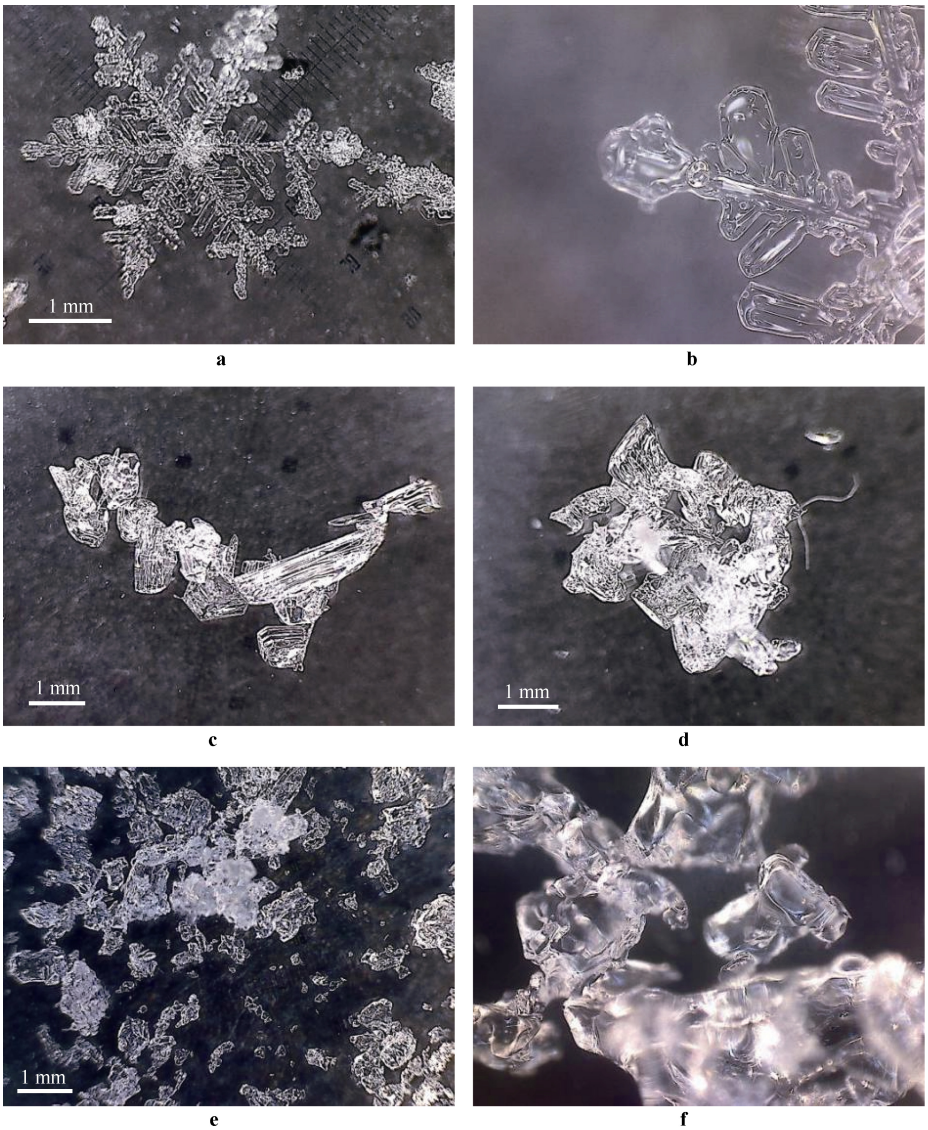


**Figure 9** Microscope images of snow particles at different stages of aging. **a**, Freshly fallen snow particle; **b**, Structural details of dendrites; **c** and **d,** Snow particle after compaction; **e**, Snow particle 168 h later; **f**, Formation of bonds between grains 168 h later.

Figure 9a shows the particles of natural snowfall, collected during the snowfall process. The dendrites of the snow particle can be clearly seen in the picture. Paterson (1994) showed that as soon as snowflakes hit the surface, the free energy of the system tends towards a minimum, such that dendritic and irregularly shaped crystals with a large surface area are gradually transformed to rounded particles. This reduction in surface energy of the system is the primary driving force for the process of sintering. Sintering is defined as "a thermal treatment for bonding particles into a coherent, predominantly solid structure via mass transport events that often occur on the atomic scale" (Blackford, 2007). Because the radius of an ice particle is larger than the concave radius of the bond joining it to an adjacent ice particle, there is a driving force to move mass to this concave neck area. Therefore, two previously spherical particles start tending towards a "dumbbell" shaped particle joined by a neck. As shown in Figure 9f, the bonds have become quite strong after 168 h of sintering. The stronger bonding leads to a stronger system with lower energy. When this process occurs under additional pressure such as the influence of the overburden pressure, it is termed pressure sintering, and the rate of sintering is increased (McCallum, 2012). In this case, several snow particles were compacted together without bonds, the dendritic and irregular shapes of the compacted snow particles have become more rounded, and their size is much smaller than that of the particle in Figure 9a.

However, the results of Table 2 reveal that the penetration pressure of the 168-h-old snow is slightly lower than that of the 120-h-old snow. This may be caused by the non-uniform conditions under which some of the tests were conducted, such as diurnal temperature fluctuations which may lead to temperature gradients within the wooden boxes.

The strength is also dependent on the overall snow temperature; usually the warmer the snowpack, the weaker it becomes, and vice versa (Schweizer et al., 2003). Additionally, while sintering near the melting point occurs rapidly and the results in rapid snow strength increase (Ramseier, 1967), below –4℃ sintering occurs significantly more slowly (Abele and Frankenstein, 1967). Although there are no continuous temperature observations, available temperature data show that the temperature during tests 73–74 was higher than that during tests 71–72. We assume that the sintering speeds were slow and with only small fluctuations as the temperatures were near −20℃ and did not change much. In addition, the study by Gow and Ramseier (1964) shows that temperature changes, temperature gradients and solar radiation all have important effects on snow metamorphosis. The effects of these variables and of variable degrees of compaction on the age-hardening properties of snow in long time sequences merit further laboratory study. Overall, the results to date suggest that optimum strengthening would be obtained with time and that the cone penetrometer is a useful and convenient instrument for monitoring the age hardening process of snow.

# 5 Conclusions

The Rammsonde was designed for use in the polar environment; the size and weight of its components make it inadequate for use on seasonal snow, whose density and hardness are lower. Therefore, some modification of the size and weight of the penetrator were made. Compared with previous models, the modified Rammsonde is lighter overall, with improved resolution, thus more suitable for seasonal snow; the mechanical structure was adjusted, and the reading of the depth data is more convenient. The preliminary evaluation of the modified cone penetrometer demonstrated that it is capable of assessing the strength of layered compacted seasonal snow. For snow with densities ranging from low to high (400–600 $kg \cdot m^{-3}$), the penetration resistance was quantified so that it was used as an index for a qualitative assessment of the mechanical behavior of snow. A series of comparative tests revealed that the assessment of the strength of layered compacted seasonal snow via the modified cone penetrometer was affected by many factors, including confining pressure, penetration energy and snow material properties, particularly the compaction degree of the snow undergoing penetration. A linear relationship between the penetration pressure and density of snow was established, and analysis of microscope images suggests that this was due to variation in the snow's internal structure. The effect of age hardening on the penetration pressure was studied and the microstructure of snow particles at different stages of aging was observed through a microscope. These tests showed that the cone penetrometer provided a rapid estimate of the snow strength. However, the effects of many variables, such as variations of ambient temperature, merit further laboratory study. Also, the use of the modified penetrometer for snow measurements requires further improvement as the vertical and resistance resolution of the cone penetrometer were too coarse to capture thin weak layers and small hardness variations in soft snow layers. Therefore, a constant-speed, high resolution penetrometer driven by an electromotor is being developed. Its effectiveness and applicability have yet to be tested in seasonal snow, prior to a possible application in Antarctica, after further verification and improvements.

**Acknowledgments** This research was supported by the National Natural Science Foundation of China (Grant nos. 41676187 and 41876213). We appreciate very much the reviewer Adrian McCallum, one anonymous reviewer and Associate Editor Jon-Ove Hagen for their helpful and constructive comments on the manuscript of this paper.

## References

Abele G. 1990. Snow Roads and Runways. CRREL Technical Report 90-3. U.S. Army Cold Regions Research and Engineering Laboratory, Hanover, NH.

Abele G, Frankenstein G. 1967. Snow and ice properties as related to roads and runways in Antarctica. CRREL Technical Report 176. U.S. Army Cold Regions Research and Engineering Laboratory, Hanover, NH.

Bader H, Haefeli R, Bucher E, et al. 1939. Der Schnee und seine Metamorphose. Beitrage zur Geologie der Schweiz. Schweizerische Schnee-und Lawinenforschungskommission (Snow and Its Metamorphism). SIPRE Trans, 14, 1954.

Blackford J R. 2007. Sintering and microstructure of ice: a review. Phys D Appl Phys, 40(21): 355-385, doi: 10.1088/0022-3727/40/21/R02.

Blaisdell G L, Lang R M, Crist G, et al. 1998. Construction, maintenance, and operation of a glacial runway, McMurdo Station, Antarctica. Monograph 98-1, U.S. Army Cold Regions Research and Engineering Laboratory, Hanover, NH.

Borstad C P, McClung D M. 2011. Thin-blade penetration resistance and snow strength. J Glaciol, 57(202): 325-336, doi: 10.3189/002214311796405924.

Bull C. 1956. The use of the Rammsonde as an instrument for determining the density of firn. J Glaciol, 2(20): 714-718, doi: 10.3189/S0022143000024941.

Colbeck S C. 1987. Snow metamorphism and classification. Nato Asi, 211: 1-35, doi:10.1007/978-94-009-3947-9_1.

Fukue M. 1977. Mechanical performance of snow under loading. PhD thesis, McGill University.

Gao S J, Hao W F, Li F, et al. 2018. Progress in application of airborne gravity measurements in polar regions. Chin J Polar Res, 30(1): 97-113.

Gow A J, Ramseier R O. 1964. Age hardening of snow at the South Pole. J Glaciol, 4(35): 521-536, doi: 10.1017/S0022143000028069.

Gubler H U. 1975. On the Rammsonde hardness equation. Proceedings of the Grindelwald Symposium (1974), IAHS Publ, 114: 110-121.

Hong W, Wei W S, Liu M Z, et al. 2014. Metamorphism and microstructure of seasonal snow: single layer tracking in western

Tianshan, China. J Mt Sci, 11(2): 496-506, doi: 10.1007/s11629-013-2815-1.

Kirchner H O K, Michot G, Narita H, et al. 2001. Snow as a foam of ice: plasticity, fracture and the brittle-to-ductile transition. Philos Mag, 81(9): 2161-2181, doi: 10.1080/01418610108217141.

Martin D C. 1997. Seventeenth Canadian geotechnical colloquium: The effect of cohesion loss and stress path on Brittle Rock strength. Can Geotech J, 34(5): 698-725, doi: 10.1139/t97-030.

McCallum A. 2012. Cone penetration testing in polar snow. PhD thesis, University of Cambridge.

McCallum A. 2014. Cone penetration testing (CPT) in Antarctic firn: an introduction to interpretation. J Glaciol, 60(219): 83-93, doi: 10.3189/2014jog12j214.

McCallum A. 2018. Polar science needs a foundation: where is the research into polar infrastructure? Adv Polar Sci, 2018, 29 (1): 1-2, doi: 10.13679/j.advps.2018.1.00001.

Melendy T D, Shoop S A. 2017. 2010/11 McMurdo Station snow-road strength and maintenance. ERDC/CRREL TR-17-3. U.S. Army Cold Regions Research and Engineering Laboratory, Hanover, NH.

Mellor M. 1975. A review of basic snow mechanics. snow mechanics (Proceedings of the Grindelwald Symposium, April 1974), IAHS Publ, 114: 251-291.

Moser E H, Sherwood G E. 1967. The load-carrying capacity of depth-processed snow on deep snowfields. Physics of Snow and Ice: Proceedings, 1(2): 993-1005.

Niedringhaus L. 1965. Study of the Rammsonde for use in hard snow. CRREL Technical Report 153. U.S. Army Cold Regions Research and Engineering Labor, Hanover, NH.

Paterson W S B. 1994. The physics of glaciers, 3rd ed., Elsevier Science Ltd., Oxford.

Petrovic J J. 2003. Review mechanical properties of ice and snow. J Mater Sci, 38(1): 1-6, doi: 10.1023/a:1021134128038.

Perla R I, Martinelli M J. 1975. Avalanche Handbook. U. S. Department of Agriculture, Agriculture Handbook 489.

Ramseier R O. 1967. Role of sintering in snow construction. CRREL Research Report 214. U.S. Army Cold Regions Research and Engineering Labor, Hanover, NH.

Renshaw C E, Schulson E M. 2001. Universal behaviour in compressive failure of brittle materials. Nature, 412(6850): 897-900, doi: 10.1038/35091045.

Schaerer P A, McClung D. 2006. The avalanche handbook: 3rd Edition. Seattle, WA: Mountaineers Books.

Schneebeli M, Johnson J B. 1998. A constant-speed penetrometer for high-resolution snow stratigraphy. Ann Glaciol, 26: 107-111, doi: 10.3189/1998aog26-1-107-111.

Schweizer J, Jamieson J B, Schneebeli M. 2003. Snow avalanche formation. Rev Geophys, 41(4): 1016, doi: 10.1029/2002rg000123.

Shapiro L H, Johnson J B, Sturm M, et al. 1997. Snow mechanics: review of the state of knowledge and applications. CRREL Report 97-3. U.S. Army Cold Regions Research and Engineering Labor, Hanover, NH.

Shoop S A, Knuth M A, Wieder W L, et al. 2014. Vehicle impact testing of snow roads at McMurdo Station, Antarctica. ERDC/CRREL TR-14-9. U.S. Army Cold Regions Research and Engineering Laboratory, Hanover, NH.

Shoop S A, Phetteplace G, Wieder W L. 2010. Snow roads at McMurdo Station, Antarctica. ERDC/CRREL TR-10-5. U.S. Army Cold Regions Research and Engineering Laboratory, Hanover, NH.

Sun Q Z, Zhang L, Qin T, et al. 2016. A review of operational weather services for fixed-wing aircrafts in Antarctica. Chin J Polar Res, 28(3): 400-412.

Swinkels L J. 2017. Stress distribution calculations through a snow slab of varying hardness: comparision with stability evalution in the field. Master thesis, The Arctic University of Norway.

Waterhouse R W. 1966. Re-evaluation of the Rammsonde hardness equation. J Glaciol, 6(45): 425-430, doi: 10.1017/S0022143000019547.

Wong J Y, Irwin G J. 1992. Measurement and characterization of the pressure-sinkage data for snow obtained using a Rammsonde. J Terramechanics, 29(2): 265-280, doi: 10.1016/0022-4898(92)90031-E.

Wuori A F. 1963. Snow stabilization for roads and runways. CRREL Technical Report 83. U.S. Army Cold Regions Research and Engineering Labor, Hanover, NH.

Xu C, Meng S, Li Y S, et al. 2012. The weather condition for aviation at Antarctic Zhongshan Station. Marine Forecasts, 29(1): 55-59, doi: 10.1053/ejvs.2002.1857.

**Appendix Table 1** Specific test groups and detailed information

| Test | Date | Ambient temperature /℃ | Snow temperature /℃ | Average density /(kg·m$^{-3}$) | Penetration energy | Dimensions of wooden boxes/m |
|---|---|---|---|---|---|---|
| 1 | 19/1/2018 | −10.4 | −8.9 | 550 | 2 kg, 10 cm | 0.15×0.15×0.6 |
| 2 | 19/1/2018 | −11 | −11.2 | 550 | 2 kg, 10 cm | 0.15×0.15×0.6 |
| 3 | 20/1/2018 | −17.1 | −17.2 | 550 | 2 kg, 10 cm | 0.15×0.15×0.6 |
| 4 | 20/1/2018 | −14.8 | −13.7 | 550 | 2 kg, 10 cm | 0.15×0.15×0.6 |
| 5 | 20/1/2018 | −13.3 | −11.9 | 550 | 2 kg, 10 cm | 0.15×0.15×0.6 |
| 6 | 20/1/2018 | −10.6 | −9.1 | 550 | 2 kg, 20 cm | 0.15×0.15×0.6 |
| 7 | 20/1/2018 | −11 | −10.1 | 550 | 2 kg, 20 cm | 0.15×0.15×0.6 |
| 8 | 20/1/2018 | −13.5 | −12.5 | 550 | 2 kg, 20 cm | 0.15×0.15×0.6 |
| 9 | 4/2/2018 | −19.5 | −20.2 | 500 | 2 kg, 10 cm | 0.25×0.25×0.6 |
| 10 | 4/2/2018 | −19.6 | −20.3 | 500 | 2 kg, 10 cm | 0.25×0.25×0.6 |
| 11 | 4/2/2018 | −19.5 | −17.5 | 500 | 2 kg, 10 cm | 0.25×0.25×0.6 |
| 12 | 4/2/2018 | −18.5 | −16.9 | 500 | 2 kg, 10 cm | 0.25×0.25×0.6 |
| 13 | 4/2/2018 | −15.8 | −13.7 | 500 | 2 kg, 10 cm | 0.25×0.25×0.6 |
| 14 | 31/1/2018 | −11.8 | −16.1 | 500 | 2 kg, 10 cm | 0.15×0.15×0.6 |
| 15 | 31/1/2018 | −10.1 | −14.1 | 500 | 2 kg, 10 cm | 0.15×0.15×0.6 |
| 16 | 31/1/2018 | −13.7 | −13.2 | 500 | 2 kg, 10 cm | 0.15×0.15×0.6 |
| 17 | 31/1/2018 | −13.6 | −13.1 | 500 | 2 kg, 10 cm | 0.15×0.15×0.6 |
| 18 | 31/1/2018 | −15.6 | −12.9 | 500 | 2 kg, 10 cm | 0.15×0.15×0.6 |
| 19 | 4/2/2018 | −16.3 | −14.5 | 500 | 2 kg, 10 cm | 0.09×0.09×0.6 |
| 20 | 4/2/2018 | −16.6 | −14.7 | 500 | 2 kg, 10 cm | 0.09×0.09×0.6 |
| 21 | 4/2/2018 | −17.1 | −14 | 500 | 2 kg, 10 cm | 0.09×0.09×0.6 |
| 22 | 4/2/2018 | −19.4 | −15.4 | 500 | 2 kg, 10 cm | 0.09×0.09×0.6 |
| 23 | 4/2/2018 | −20.4 | −16.6 | 500 | 2 kg, 10 cm | 0.09×0.09×0.6 |
| 24 | 29/1/2018 | −15.9 | −17.7 | 450 | 1 kg, 15 cm | 0.15×0.15×0.6 |
| 25 | 29/1/2018 | −15.9 | −18.5 | 450 | 1 kg, 15 cm | 0.15×0.15×0.6 |
| 26 | 29/1/2018 | −18 | −13.3 | 450 | 1 kg, 15 cm | 0.15×0.15×0.6 |
| 27 | 29/1/2018 | −18.9 | −17 | 450 | 1 kg, 15 cm | 0.15×0.15×0.6 |
| 28 | 29/1/2018 | −19 | −16.6 | 450 | 1 kg, 15 cm | 0.15×0.15×0.6 |
| 29 | 29/1/2018 | −19.2 | −14.5 | 450 | 1 kg, 20 cm | 0.15×0.15×0.6 |
| 30 | 30/1/2018 | −18.5 | −19.6 | 450 | 1 kg, 20 cm | 0.15×0.15×0.6 |
| 31 | 30/1/2018 | −16.2 | −17.5 | 450 | 1 kg, 20 cm | 0.15×0.15×0.6 |
| 32 | 30/1/2018 | −14.8 | −13.1 | 450 | 1 kg, 20 cm | 0.15×0.15×0.6 |
| 33 | 30/1/2018 | −13.6 | −13.3 | 450 | 1 kg, 20 cm | 0.15×0.15×0.6 |
| 34 | 30/1/2018 | −12.2 | −13.9 | 450 | 1 kg, 25 cm | 0.15×0.15×0.6 |
| 35 | 30/1/2018 | −13.8 | −9.5 | 450 | 1 kg, 25 cm | 0.15×0.15×0.6 |
| 36 | 30/1/2018 | −14.1 | −11.2 | 450 | 1 kg, 25 cm | 0.15×0.15×0.6 |
| 37 | 30/1/2018 | −15.1 | −11.3 | 450 | 1 kg, 25 cm | 0.15×0.15×0.6 |
| 38 | 30/1/2018 | −14.2 | −10.5 | 450 | 1 kg, 25 cm | 0.15×0.15×0.6 |
| 39 | 30/1/2018 | −15.1 | −10.2 | 450 | 1 kg, 30 cm | 0.15×0.15×0.6 |
| 40 | 30/1/2018 | −15.1 | −11.5 | 450 | 1 kg, 30 cm | 0.15×0.15×0.6 |
| 41 | 30/1/2018 | −15.5 | −11.1 | 450 | 1 kg, 30 cm | 0.15×0.15×0.6 |
| 42 | 30/1/2018 | −15.9 | −11 | 450 | 1 kg, 30 cm | 0.15×0.15×0.6 |
| 43 | 30/1/2018 | −16.1 | −11.5 | 450 | 1 kg, 30 cm | 0.15×0.15×0.6 |
| 44 | 1/2/2018 | −13.5 | −12.3 | 500 | 2 kg, 15 cm | 0.15×0.15×0.6 |

Continued

| Test | Date | Ambient temperature /℃ | Snow temperature /℃ | Average density /(kg·m$^{-3}$) | Penetration energy | Dimensions of wooden boxes/m |
|---|---|---|---|---|---|---|
| 45 | 1/2/2018 | −12.1 | −11 | 500 | 2 kg, 15 cm | 0.15×0.15×0.6 |
| 46 | 1/2/2018 | −12.4 | −11.9 | 500 | 2 kg, 15 cm | 0.15×0.15×0.6 |
| 47 | 1/2/2018 | −11.2 | −11.3 | 500 | 2 kg, 15 cm | 0.15×0.15×0.6 |
| 48 | 1/2/2018 | −10.8 | −10.1 | 500 | 2 kg, 15 cm | 0.15×0.15×0.6 |
| 49 | 1/2/2018 | −10.4 | −10.6 | 500 | 2 kg, 20 cm | 0.15×0.15×0.6 |
| 50 | 1/2/2018 | −10.7 | −10.2 | 500 | 2 kg, 20 cm | 0.15×0.15×0.6 |
| 51 | 1/2/2018 | −9.8 | −12.9 | 500 | 2 kg, 20 cm | 0.15×0.15×0.6 |
| 52 | 1/2/2018 | −10.3 | −11.9 | 500 | 2 kg, 20 cm | 0.15×0.15×0.6 |
| 53 | 1/2/2018 | −9.2 | −10.2 | 500 | 2 kg, 20 cm | 0.15×0.15×0.6 |
| 54 | 31/1/2018 | −14.9 | −12.6 | 400 | 2 kg, 10 cm | 0.15×0.15×0.6 |
| 55 | 31/1/2018 | −15.2 | −13.1 | 400 | 2 kg, 10 cm | 0.15×0.15×0.6 |
| 56 | 31/1/2018 | −15.6 | −13.6 | 400 | 2 kg, 10 cm | 0.15×0.15×0.6 |
| 57 | 31/1/2018 | −16.7 | −15 | 400 | 2 kg, 10 cm | 0.15×0.15×0.6 |
| 58 | 31/1/2018 | −16.7 | −15 | 400 | 2 kg, 10 cm | 0.15×0.15×0.6 |
| 59 | 31/1/2018 | −18.5 | −20 | 450 | 2 kg, 10 cm | 0.15×0.15×0.6 |
| 60 | 31/1/2018 | −16.8 | −20.1 | 450 | 2 kg, 10 cm | 0.15×0.15×0.6 |
| 61 | 31/1/2018 | −16.1 | −20 | 450 | 2 kg, 10 cm | 0.15×0.15×0.6 |
| 62 | 31/1/2018 | −13.9 | −16.4 | 450 | 2 kg, 10 cm | 0.15×0.15×0.6 |
| 63 | 31/1/2018 | −14.1 | −17.9 | 450 | 2 kg, 10 cm | 0.15×0.15×0.6 |
| 64 | 2/2/2018 | −10.1 | −13 | 600 | 2 kg, 10 cm | 0.15×0.15×0.6 |
| 65 | 2/2/2018 | −12.4 | −12.6 | 600 | 2 kg, 10 cm | 0.15×0.15×0.6 |
| 66 | 3/2/2018 | −14.8 | −13.5 | 600 | 2 kg, 10 cm | 0.15×0.15×0.6 |
| 67 | 3/2/2018 | −19 | −17.6 | 600 | 2 kg, 10 cm | 0.15×0.15×0.6 |
| 68 | 3/2/2018 | −18.6 | −17 | 600 | 2 kg, 10 cm | 0.15×0.15×0.6 |
| 69 | 22/1/2018 – 25/1/2018 | −22.4/−20.5 | −18.2/−19.2 | 500 | 2 kg, 20 cm | 0.15×0.15×0.6 |
| 70 | 22/1/2018 – 25/1/2018 | −20/−19.2 | −19/−19.2 | 500 | 2 kg, 20 cm | 0.15×0.15×0.6 |
| 71 | 22/1/2018 – 27/1/2018 | −22.8/−20.8 | −18.4/−16.5 | 500 | 2 kg, 20 cm | 0.15×0.15×0.6 |
| 72 | 22/1/2018 – 27/1/2018 | −19/−21.1 | −20.2/−19.5 | 500 | 2kg, 20 cm | 0.15×0.15×0.6 |
| 73 | 28/1/2018 – 4/2/2018 | −20.4/−14.8 | −18.3/−14.3 | 500 | 2kg, 20 cm | 0.15×0.15×0.6 |
| 74 | 28/1/2018 – 4/2/2018 | −20.2/−14.3 | −18.8/−13.6 | 500 | 2kg, 20 cm | 0.15×0.15×0.6 |

Notes: For Tests 69–74, no continuous temperature measurements were carried out during outdoor placement. The temperatures listed were those measured before the snow sample preparation and the penetration test.